Helix-Sense Inversion of Poly(phenylacetylene) Derivatives Bearing an Optically Active Substituent Induced by External Chiral and Achiral Stimuli

Kazuhide Morino, Katsuhiro Maeda, and Eiji Yashima*

Department of Molecular Design and Engineering, Graduate School of Engineering, Nagoya University, Chikusa-ku, Nagoya 464-8603, Japan

Received October 9, 2002; Revised Manuscript Received December 31, 2002

ABSTRACT: Novel, optically active, *cis*−*transoidal* poly(phenylacetylenes), poly((*R*)-(−)- or (*S*)-(+)-(4-((1-(1-naphthyl)ethyl)carbamoyl)phenyl)acetylene) (poly(*R*)-**1** and poly(*S*)-**1**), were prepared, and their chiroptical properties were investigated by means of circular dichroism spectroscopy. We have found that the poly-**1**'s have a predominant one-handed helical conformation in solution, and the helix-sense undergoes a transition from one helix to another in response to external, chiral, and achiral stimuli, such as temperature, solvent, and chiral interaction with small molecules.

Introduction

Optically active helical polymers have aroused considerable interest from many viewpoints including syntheses, structures, and functions.[1] We recently found that stereoregular *cis*−*transoidal* poly(phenylacetylene) derivatives bearing various functional groups such as poly((4-carboxyphenyl)acetylene) form an induced one-handed helical structure upon complexation with optically active compounds capable of interacting with the functional groups of the poly(phenylacetylenes).[2] The complexes show an induced circular dichroism (ICD) in the UV−vis region, probably due to the prevailing one-handed helix formation of the polymer backbone upon complexation with optically active compounds. The Cotton effect signs can be used as a probe for the chirality assignment of the chiral compounds. More interestingly, the macromolecular helicity induced on poly((4-carboxyphenyl)acetylene) (PCPA) with chiral amines, for instance (*R*)-(+)-1-(1-naphthyl)ethylamine ((*R*)-**2**), was found to be "*memorized*" when the chiral amine was replaced by various achiral amines.[3] To elucidate the mechanism of this unique helicity induction and memory process, novel, optically active poly(phenylacetylenes), poly((*R*)-(−)- or (*S*)-(+)-(4-((1-(1-naphthyl)ethyl)carbamoyl)phenyl)acetylene) (poly(*R*)-**1** and poly(*S*)-**1**) (Chart 1), were prepared, and their chiroptical properties were investigated using circular dichroism (CD) spectroscopy. Poly-**1**'s are considered as model polymers for the helicity induction of PCPA with (*R*)-**2** or (*S*)-**2** because poly-**1** has an optically active (*R*)- or (*S*)-**2** unit as the substituent through covalent bonding. We report here that poly(*R*)-**1** and poly(*S*)-**1** undergo a helix−helix transition by response to external, chiral, and achiral stimuli, such as temperature, solvent, and chiral interaction with small molecules. Although several synthetic polymers as well as biopolymers[4] are known to exhibit helix inversion between right- and left-handed helical conformations by changing the external conditions, such as solvent,[5] temperature,[6] or by the irradiation of light,[7] helicity inversion of a macromolecular helicity responding to chiral stimuli is still quite rare. Only a few optically active poly(phenylacetylenes) bearing a chiral amine, i.e., (1*R*,2*S*)-norephedrine[8] or cyclodextrin residues,[9] exhibited a helix−helix transition induced by external chiral stimuli through diastereomeric acid−base interactions or complexations with chiral guest molecules, respectively.

* Corresponding author: e-mail yashima@apchem.nagoya-u.ac.jp.

Experimental Section

Materials. Tetrahydrofuran (THF) was dried over sodium benzophenone ketyl and distilled onto calcium hydride, followed by vacuum distillation onto $LiAlH_4$ under nitrogen. Triethylamine (Et_3N) was dried over KOH pellets and distilled onto KOH under nitrogen. These solvents were distilled under high vacuum just before use. Dimethylformamide (DMF) was dried over calcium hydride and distilled under reduced pressure. Chloroform ($CHCl_3$) was dried over calcium hydride, distilled, and stored under nitrogen. 4-Ethynylbenzoic acid was prepared according to the previously reported method.[2d] 1-Hydroxybenzotriazole monohydrate (HBT) and *N*,*N*′-dicyclohexylcarbodiimide (DCC) were purchased from Wako (Osaka, Japan) and Nacalai Tesque (Kyoto, Japan), respectively. *N*-Methylmorpholine (NMM) was obtained from Kishida (Osaka, Japan). Anhydrous dimethyl sulfoxide (DMSO, water content <0.005%), anhydrous methanol (water content <0.002%), and bis[(norbornadiene)rhodium(I) chloride] {$[Rh(nbd)Cl]_2$} were purchased from Aldrich. Benzylamine and (*RS*)-1-(1-naphthyl)ethylamine were from Tokyo Kasei (Tokyo, Japan). Both (*R*)-(+)- and (*S*)-(−)-1-(1-naphthyl)ethylamine were kindly supplied from Yamakawa Chemical (Tokyo, Japan).

(*R*)-(−)-(4-((1-(1-Naphthyl)ethyl)carbamoyl)phenyl)-acetylene ((*R*)-1). 4-Ethynylbenzoic acid (500 mg, 3.42 mmol) and HBT (525 mg, 3.43 mmol) were dissolved in DMF (25 mL), and to this was added DCC (712 mg, 3.45 mmol) at 0 °C. The reaction mixture was stirred at 0 °C for 1 h and then at room temperature for 1 h. To the solution was added (*R*)-(+)-1-(1-naphthyl)ethylamine (0.66 mL, 4.1 mmol) and NMM (0.38 mL, 3.5 mmol). The reaction mixture was stirred at room temperature for 24 h. After evaporating the solvent, the residue was dissolved in THF, and the solution was poured into aqueous HCl. After the dispersion solution was stirred at room temperature for 14 h, the precipitate was collected by filtration. The crude product was purified by silica gel chromatography with $CHCl_3$ as the eluent and then recrystallization from *n*-hexane−ethyl acetate (1/1, v/v) to give 570 mg of monomer (*R*)-**1** as a white crystal in 56% yield (mp 184.0−184.5 °C). IR (Nujol): 3287 ($\nu_{\equiv CH}$), 1626 (amide I), 1525 cm^{-1} (amide II). ^1H NMR (DMSO-d_6, 300 MHz): δ 1.61 (d, CH_3, J = 7.2 Hz, 3H), 4.39 (s, ≡CH, 1H), 5.91−6.01 (m, CH, 1H), 7.47−8.21 (m,

10.1021/ma025726p CCC: $25.00
Published on Web 02/07/2003

Chart 1

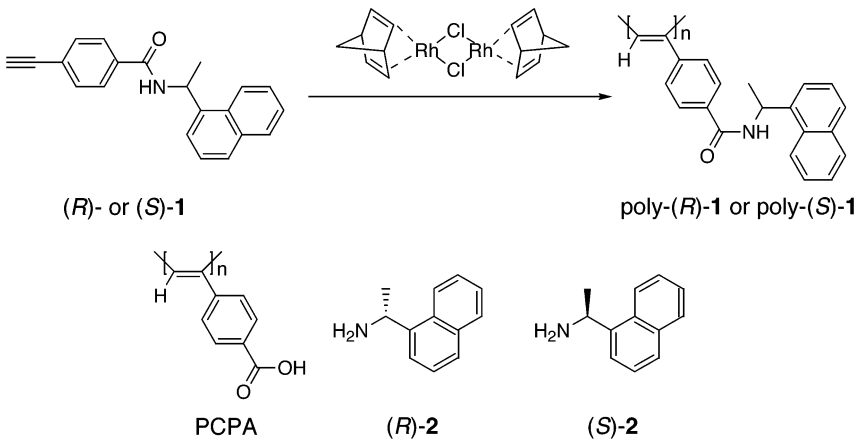

aromatic, 11H), 9.08 (d, NH, J = 7.5 Hz, 1H). ^{13}C NMR (DMSO-d_6, 75 MHz): δ 21.5, 44.8, 82.8, 82.9, 122.4, 123.0, 124.3, 125.3, 125.4, 126.1, 127.1, 127.6, 128.5, 130.2, 131.4, 133.2, 134.3, 140.1, 164.4. Anal. Calcd for $C_{21}H_{17}NO\cdot{}^1/_8H_2O$: C, 83.62; H, 5.76; N, 4.64. Found: C, 83.62; H, 5.83; N, 4.65. $[\alpha]_D^{25}$ −170° (*c* 0.5, methanol).

(*S*)-**1** was prepared in the same way using (*S*)-(−)-1-(1-naphthyl)ethylamine in 79% yield; mp 186.2−187.0 °C. IR (Nujol): 3287 ($\nu_{\equiv CH}$), 1626 (amide I), 1526 cm^{-1} (amide II). ^{1}H NMR (DMSO-d_6, 300 MHz): δ 1.60 (d, CH_3, J = 7.2 Hz, 3H), 4.36 (s, ≡CH, 1H), 5.92−6.01 (m, CH, 1H), 7.47−8.21 (m, aromatic, 11H), 9.06 (d, NH, J = 7.5 Hz, 1H). ^{13}C NMR (DMSO-d_6, 75 MHz): δ 21.4, 44.8, 82.8, 82.9, 122.5, 123.1, 124.4, 125.5, 125.6, 126.2, 127.3, 127.7, 128.7, 130.4, 131.6, 133.2, 134.4, 140.2, 164.4. Anal. Calcd for $C_{21}H_{17}NO$: C, 84.25; H, 5.30; N, 4.91. Found: C, 83.97; H, 5.35; N, 4.80. $[\alpha]_D^{25}$ +170 ° (*c* 0.5, methanol).

Polymerization. Polymerization was carried out in a dry glass ampule under a dry nitrogen atmosphere using [Rh(nbd)Cl]$_2$ as a catalyst. A typical polymerization procedure is described below (see Chart 1).

Monomer (*R*)-**1** (200 mg, 0.668 mmol) was placed in a dry glass ampule, which was then evacuated on a vacuum line and flushed with dry nitrogen. After this evacuation−flush procedure was repeated three times, a three-way stopcock was attached to the ampule and dry THF (2.3 mL) and Et_3N (0.088 mL) were added with a syringe. To this was added a solution of [Rh(nbd)Cl]$_2$ (0.005 M) in THF at 30 °C. The concentrations of the monomer and the rhodium complex were 0.2 and 0.002 M, respectively. The polymerization rapidly proceeded, and a red polymer was precipitated within a few seconds. After 0.5 h, the resulting polymer was precipitated into a large amount of methanol, collected by filtration, and dried in vacuo at 50 °C for 3 h. The obtained polymer was dissolved in a small amount of DMF, and the DMF solution was reprecipitated into methanol. The resulting yellow polymer was collected by centrifugation and dried in vacuo at 50 °C for 3 h.

Spectroscopic data of poly(*R*)-**1**. IR (Nujol): 1639 (amide I), 1525cm^{-1} (amide II). ^{1}H NMR (DMF-d_7, 80 °C, 500 MHz): δ 1.54 (d, CH_3, 3H), 5.88 (s, =CH, 1H), 5.99 (s, CH, 1H), 6.74 (s, aromatic, 2H), 7.18−8.15 (m, aromatic, 9H), 8.39 (s, NH, 1H). Anal. Calcd for $(C_{21}H_{17}NO\cdot{}^2/_3H_2O)_n$: C, 81.00; H, 5.93; N, 4.50. Found: C, 81.18; H, 5.92; N, 4.44. $[\alpha]_D^{25}$ +105° (*c* 0.5, DMF).

Spectroscopic data of poly(*S*)-**1**. IR (Nujol): 1638 (amide I), 1525 cm^{-1} (amide II). ^{1}H NMR (DMF-d_7, 80 °C, 500 MHz): δ 1.55 (d, CH_3, 3H), 5.88 (s, =CH, 1H), 5.98 (s, CH, 1H), 6.74 (s, aromatic, 2H), 7.19−8.15 (m, aromatic, 9H), 8.35 (s, NH, 1H). Anal. Calcd for $(C_{21}H_{17}NO\cdot{}^5/_9H_2O)_n$: C, 81.53; H, 5.90; N, 4.53. Found: C, 81.78; H, 5.74; N, 4.53. $[\alpha]_D^{25}$ −113° (*c* 0.5, DMF).

Instruments. Melting points were measured on a Büchi melting point apparatus and are uncorrected. IR spectra were recorded using a Jasco Fourier transform IR-620 spectrophotometer (Hachioji, Japan). Optical rotation was measured in a 2 or 5 cm quartz cell on a Jasco P-1030 polarimeter. NMR spectra were taken on a Varian Mercury 300 operating at 300 MHz for ^{1}H or a Varian VXR-500 (500 MHz for ^{1}H) spectrometer with TMS (for $CDCl_3$ and DMF-d_7) or a solvent residual peak (for DMSO-d_6) as the internal standard. The absorption and CD spectra were measured in a 0.1 cm quartz cell unless otherwise noted using a Jasco V-570 spectrophotometer and a Jasco J-725 spectropolarimeter, respectively. The temperature was controlled with a Jasco PTC-348WI apparatus. Size exclusion chromatography (SEC) was performed with a Jasco PU-980 liquid chromatograph equipped with a UV−vis (300 nm, Jasco UV-970), a RI (Jasco RI-930) detector, and a column oven (Jasco CO-965). The molecular weight (M_n) was determined at 40 °C using Tosoh TSK-GEL α-3000 (30 cm) and α-5000 (30 cm) SEC columns connected in series, and DMF containing 10 mM LiCl was used as the eluent at a flow rate of 0.5 mL/min. The molecular weight calibration curve was obtained with poly(ethylene oxide) and poly(ethylene glycol) standards (Tosoh). Laser Raman spectra were measured on a Jasco NRS-1000 spectrophotometer. Atomic force microscopy (AFM) measurements were performed on a Nanoscope IIIa microscope (Digital Instruments, Santa Barbara, CA) in air using standard silicon tips (NCH-10V) in the tapping mode. Height and phase images were simultaneously measured at the resonance frequency of the tips with 125 μm long cantilevers (235−240 kHz). All the images were collected with the maximum available number of pixels (512) in each direction (2 μm). Scanning speed was at a line frequency of 1.0 Hz. Dynamic light scattering (DLS) measurements were performed on a DLS-6600HK (Otsuka Electronics Co. Ltd., Japan) equipped with a 10 mW He−Ne Laser (632.8 nm) at a fixed scattering angle of 90° at 25 °C.

CD Measurements: Effect of Solvent on ICD of Poly-1. A typical experimental procedure is described below. A stock solution of poly(*R*)-**1** (5 mg/mL) in DMF was prepared in a 2 mL flask equipped with a stopcock. A 100 μL aliquot of the poly(*R*)-**1** solution was transferred to four 1 mL flasks equipped with a stopcock. To each flask was added DMF (900, 860, 800, and 700 μL) using a Hamilton microsyringe, and the solutions were diluted with methanol so as to keep the poly(*R*)-**1** concentration at 0.5 mg/mL. The absorption and CD spectra were taken for each flask. In a similar manner, effects of other poor solvents ($CHCl_3$ and pyridine) on ICD of poly(*R*)-**1** were investigated. The same procedure was performed in the CD measurements for poly(*S*)-**1**.

Effect of Optically Active Amines on ICD of Poly-1. A stock solution of poly(*R*)-**1** (2 mg/mL) in DMF was prepared in a 5 mL flask equipped with a stopcock. A 500 μL aliquot of the polymer solution was transferred to six 1 mL flasks equipped with a stopcock and (*R*)- and (*S*)-**2** (54, 220, and 270 μL) were directly added to the flasks. The solutions were then diluted with DMF to keep the poly(*R*)-**1** concentration at 1.0 mg/mL. The absorption and CD spectra were then taken for each flask. In the same way, the effect of (*R*)- and (*S*)-**2** on ICD of poly(*S*)-**1** in DMF was investigated.

Concentration Effect of Poly-1 on ICD. A stock solution of poly(*R*)-**1** (1 mg/mL) in DMF was prepared in a 2 mL flask

Table 1. Polymerization of (*R*)-1 with [Rh(nbd)Cl]$_2$ at 30 °C[a]

run	solvent	time (h)	yield (%)[b]	$M_n \times 10^{-5}$ [c]	M_w/M_n[c]
1[d]	THF	0.5	87	3.0	1.8
2	DMSO	3	2		
3	DMF	2	100	6.5	1.3
4[e]	DMF	2	100	6.0	1.2
5[f]	DMF	2	90	2.1	1.7

[a] Polymerized under nitrogen; [(*R*)-**1**] = 0.5 M, [(*R*)-**1**]/[Rh] = 200, [Et_3N]/[Rh] = 200. [b] Methanol-insoluble fraction. [c] Determined by SEC (poly(ethylene oxide) and poly(ethylene glycol) standards) with DMF containing LiCl (10 mM) as the eluent. [d] [(*R*)-**1**] = 0.2 M, [(*R*)-**1**]/[Rh] = 100, [Et_3N]/[Rh] = 100. [e] (*S*)-**1** was used instead of (*R*)-**1**. [f] [(*R*)-**1**] = 0.5 M, [(*R*)-**1**]/[Rh] = 10, [Et_3N]/[Rh] = 50.

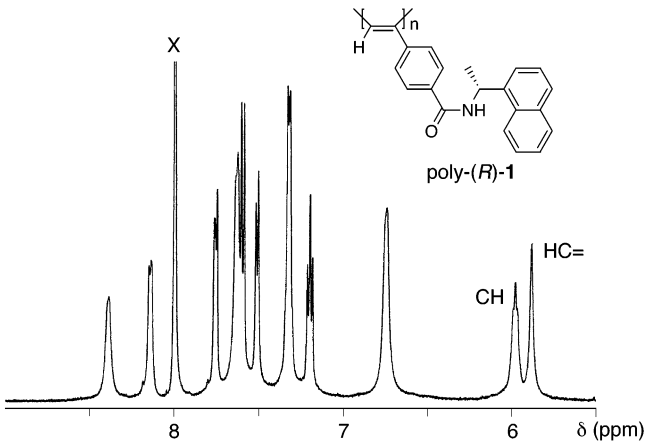

Figure 1. ^{1}H NMR spectrum of poly(*R*)-**1** (run 1 in Table 1) in DMF-d_7 at 80 °C. The X denotes protons from DMF.

equipped with a stopcock, and the initial CD spectrum was recorded with a 0.05 cm quartz cell. A 300 μL aliquot of the polymer solution was transferred to a 3 mL flask with a Hamilton microsyringe, and the solution was diluted with DMF, giving a 0.1 mg/mL solution of poly(*R*)-**1**. The CD spectrum of this solution was taken with a 0.5 cm quartz cell, and the above similar dilution procedure was repeated to prepare dilute poly(*R*)-**1** solutions (0.05 and 0.005 mg/mL). Similarly, the concentration effect of poly(*R*)-**1** on ICD in DMSO/$CHCl_3$ (1/1, v/v) was also investigated.

Results and Discussion

Synthesis and Structural Characteristics of Poly-(*R*)-1 and Poly(*S*)-1. Poly(*R*)-**1** and poly(*S*)-**1** were prepared by polymerization of the corresponding monomers with [Rh(nbd)Cl]$_2$[2,3,10] in various solvents. The results of the polymerization are summarized in Table 1. In THF, the polymerization rapidly proceeded, and a polymer precipitated within a few seconds, whereas the polymerization proceeded homogeneously in DMF to quantitatively afford high molecular weight polymers. The resulting polymers were soluble in DMF and a DMSO−$CHCl_3$ mixture (1/1, v/v) but insoluble in THF, $CHCl_3$, acetonitrile, DMSO, and acetone. However, the lower molecular weight poly(*R*)-**1** (run 5 in Table 1) was partially soluble in $CHCl_3$. On the other hand, the polymerization hardly occurred in DMSO, and only a trace amount of a methanol insoluble polymer was obtained (run 2 in Table 1).

The stereoregularity of the poly-**1**'s was investigated by ^{1}H NMR spectroscopy. The ^{1}H NMR spectrum of the poly(*R*)-**1** (run 1 in Table 1) in DMF-d_7 (Figure 1) showed a sharp singlet centered at 5.88 ppm due to the main chain protons, which can be assigned to the *cis−transoidal* main chain's olefinic protons.[11] A similar ^{1}H NMR spectrum was observed in DMSO-d_6−$CDCl_3$ (1/1, v/v). In addition, the laser Raman spectra of the polymer measured in the solid state showed characteristic peaks at 1354 and 977 cm^{-1} due to the C−C and C−H bond vibrations in the *cis*-polyacetylenes, respectively,[12] while those in the *trans*-polyacetylene were not observed. These results indicated that the poly(*R*)-**1** possesses a highly *cis−transoidal* stereoregular structure. Other polymers including poly(*S*)-**1** also showed similar ^{1}H NMR and Raman spectra, indicating high stereoregularity.

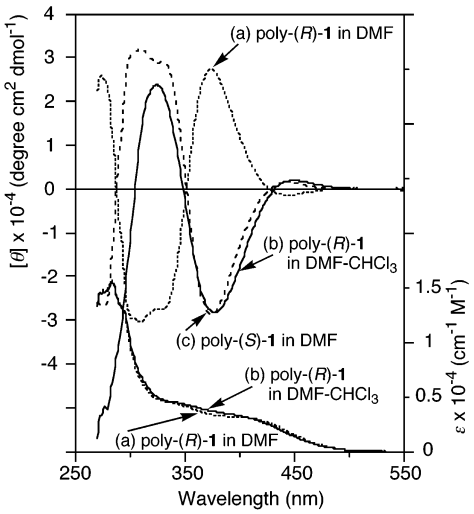

Figure 2. CD and absorption spectra of poly(*R*)-**1** (run 1 in Table 1) in DMF (a) and DMF−$CHCl_3$ (1/1, v/v) (b). The CD and absorption spectra were measured in a 0.1 cm quartz cell at ambient temperature (ca. 25−26 °C) with a poly(*R*)-**1** concentration of 0.5 mg/mL. The CD spectrum of poly(*S*)-**1** (run 4 in Table 1) in DMF is also shown in (c).

Chiroptical Property of Poly-1 and Helix-Sense Inversion. To characterize the chiroptical properties of the optically active polyacetylenes bearing a chiral substituent, CD spectroscopy is suitable for detecting macromolecular asymmetry. The CD and absorption spectra of poly(*R*)-**1** and poly(*S*)-**1** were then measured. Figure 2a shows the typical CD and absorption spectra of poly(*R*)-**1** in DMF (run 1 in Table 1). The polymer exhibited an intense, split-type ICD in the long absorption region of the conjugated polyene backbone. Poly-(*S*)-**1** also showed similar Cotton effects with complete mirror images to those of poly(*R*)-**1** (Figure 2c). The monomers (*R*)-**1** and (*S*)-**1** showed no CD band at wavelengths greater than 320 nm. This indicates that poly(*R*)-**1** and poly(*S*)-**1** have a predominantly one-handed helical conformation induced by the covalent-bonded chiral pendants. Unfortunately, the poly-**1**'s are not soluble in DMSO in which PCPA forms an induced helix with chiral amines, but poly-**1**'s were soluble in DMF and exhibited ICDs. The Cotton effects are similar in pattern to those of the *cis−transoidal* PCPA complexed with optically active amines including (*R*)-**2**[2] and poly(phenylacetylenes) with an optically active substituent at the *para* position, as previously reported,[13] but the sign of the PCPA−(*R*)-**2** complex was opposite compared with that of poly(*R*)-**1** in DMF, although the CD intensity of the PCPA−(*R*)-**2** complex was much weaker than that in DMSO (Table 2). This implies that the PCPA complexed with (*R*)-**2** has a slightly excess of a single-handed helical conformation and the helix-sense

Table 2. CD and Absorption Spectral Data of Poly(*R*)-1 (Run 1 in Table 1), Poly(*S*)-1 (Run 4 in Table 1), and PCPA−(*R*)-2 Complex in Various Solvents[a]

		poly(*R*)-**1**		poly(*S*)-**1**		PCPA−(*R*)-**2**[b]	
run	solvent	ϵ_{400}	$[\theta]_{2nd} \times 10^{-4}$ (λ)	ϵ_{400}	$[\theta]_{2nd} \times 10^{-4}$ (λ)	ϵ_{400}	$[\theta]_{2nd} \times 10^{-4}$ (λ)
1	DMF	3150	2.74 (374)	3270	−2.87 (375)	3020	−0.13 (372)
2	DMF−$CHCl_3$ (1/1)	3280	−2.83 (377)	3480	2.77 (378)	3000[c]	−0.05 (376)[c]
3	DMF−methanol (8/2)	3240	−1.97 (378)	3460	2.17 (379)	2940	−0.65 (375)
4	DMF−pyridine (1/9)	3220	−3.21 (378)	3270	3.24 (377)	3010[c]	−0.16 (375)[c]
5	DMSO−$CHCl_3$ (1/1)	3440[d]	−1.93 (378)[d]	3410[d]	1.96 (378)[d]	2870[c]	−0.61 (378)[c]
6	DMSO	*e*	*e*	*e*	*e*	2940	−3.11 (376)

[a] CD and absorption spectra were measured in a 0.1 cm quartz cell at ambient temperature (ca. 25−26 °C) with a poly-**1** concentration of 0.5 mg/mL; ϵ_{400} (cm^{-1} M^{-1}), $[\theta]$ (deg cm^2 $dmol^{-1}$) of the second Cotton, and λ (nm). [b] CD and absorption spectra were measured in a 0.05 cm quartz cell with a PCPA concentration of 1 mg/mL (6.8 mM). The concentration of (*R*)-**2** was 340 mM. [c] [PCPA] = 0.25 mg/mL. [d] CD and absorption spectra were measured in a 0.05 cm quartz cell with a poly-**1** concentration of 1 mg/mL. [e] Insoluble in DMSO.

is opposite to that of poly(*R*)-**1** bearing the same (*R*)-**2** residue covalently at least in DMF.

However, interestingly, the ICD pattern of the poly-**1**'s is almost completely inverted in DMF containing a poor solvent, such as $CHCl_3$ (DMF−$CHCl_3$ (1/1, v/v)) at ambient temperature (ca. 25−26 °C), resulting in an almost mirror image (Figure 2b). This suggests that the predominant helix-sense of the polymer may be opposite in DMF and DMF−$CHCl_3$ (1/1, v/v). The changes in the ICDs were accompanied by a negligible change in their absorption spectra. Similar helix−helix transitions also occurred for other helical polyacetylenes, polyisocyanates, and polysilanes in response to solvent,[5] temperature,[6] and chirality,[8,9] and such transitions are considered to originate from the difference in entropy between the right- and left-handed helices generated by the changes in solvation, structures of the side chains and the main chains, and intra- and intermolecular interactions, although the exact mechanism is still obscure.[5−9] Similar inversion of the Cotton effect sign was also observed in other solvent mixtures and also for poly(*S*)-**1** (Table 2). PCPA complexed with (*R*)-**2** did not show such CD changes in DMSO in the presence of poor solvents such as toluene, $CHCl_3$, and acetonitrile[2d] and in DMF containing $CHCl_3$, methanol, and pyridine (see Table 2); therefore, it is concluded that the helix−helix transition of macromolecules accompanied by inversion of the optical activity (CD and optical rotation) is a characteristic feature for helical polymers in which the optically active pendants are covalently bonded.

Another possible explanation for the helix inversion of the poly-**1**'s accompanied by the Cotton effect inversion depending on the solvent may be due to aggregations of the polymer main chains in the presence of poor solvents.[14] It is well-known that aggregations are highly sensitive to the concentration of polymers. However, the magnitudes of the ICDs of poly(*R*)-**1** in DMF, DMF−pyridine (1/9, v/v), and DMSO−$CHCl_3$ (1/1, v/v) were hardly changed over the concentration range of poly-(*R*)-**1** from 1 to 0.005 mg/mL, indicating that the formation of aggregates could be excluded.[9,15] Filtration experiments[16] of a poly(*R*)-**1** solution also support this speculation. The DMF, DMF−pyridine (1/9, v/v), and DMSO−$CHCl_3$ (1/1, v/v) solutions of poly(*R*)-**1** (1 mg/mL, run 1 in Table 1) were filtered through the membrane filter with a pore size of 0.02 μm, and the CD and absorption spectra of the filtrates were measured, but the spectra did not change after the filtration. These results indicated that the CD inversion of poly-(*R*)-**1** between the DMF, DMF−pyridine (1/9, v/v), and DMSO−$CHCl_3$ (1/1, v/v) solutions was not due to aggregation of the polymer chains.[17] AFM analyses of poly-(*R*)-**1** and poly(*S*)-**1** on a freshly cleaved mica surface also support this speculation; individual poly(*R*)-**1** and poly(*S*)-**1** chains can be directly visualized on mica prepared from a solution of poly(*R*)-**1** and poly(*S*)-**1** (0.025 mg/mL) in DMF and poly(*R*)-**1** (0.005 mg/mL) in DMF−pyridine (1/9, v/v) (see Supporting Information).[18]

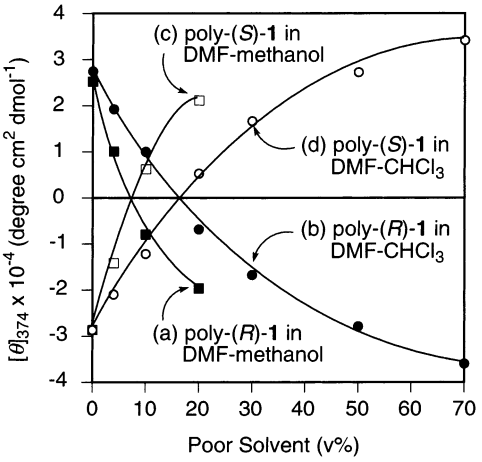

Figure 3. Changes in CD intensity of poly(*R*)-**1** (run 1 in Table 1) (a (■), b (●)) and poly(*S*)-**1** (run 4 in Table 1) (c (□), d (○)) at 374 nm in DMF−methanol (a (■), c (□)) and DMF−$CHCl_3$ (b (●), d (○)) mixtures at ambient temperature (ca. 25−26 °C). The concentration of poly-**1** was 0.5 mg/mL.

The CD titrations of poly(*R*)-**1** and poly(*S*)-**1** in DMF with increasing volumes of a poor solvent such as $CHCl_3$ and methanol were then performed to obtain an insight into the helix inversion of poly-**1** depending on the solvent composition. Figure 3 shows the changes in the $[\theta]$ value at 374 nm in DMF−poor solvent mixtures at ambient temperature. The ICD intensity significantly changed with an increase in the composition of methanol and $CHCl_3$, and the sign became inverted from the positive to negative direction for poly(*R*)-**1** and from negative to positive for poly(*S*)-**1** with clear isosbestic-like points at 430 and 351 nm to yield almost mirror images in the presence of 10 and 20 vol % methanol and $CHCl_3$, respectively. The CD spectral changes are independent of the poly(*R*)-**1** concentration (for instance, 0.5−0.025 mg/mL in DMF containing 4, 10, and 20 vol % of methanol), indicating that the formation of aggregates by the addition of poor solvents can be negligible. These results demonstrate that the poly-**1**'s undergo a transition from one helix to another in DMF−methanol or DMF−$CHCl_3$ mixtures. These significant changes in the ICDs were accompanied by a slight change in their absorption spectra; the absorption spectra exhibited a small red shift indicating that the poly-**1**'s may have a slightly loose helical conformation in the solvent mixtures.

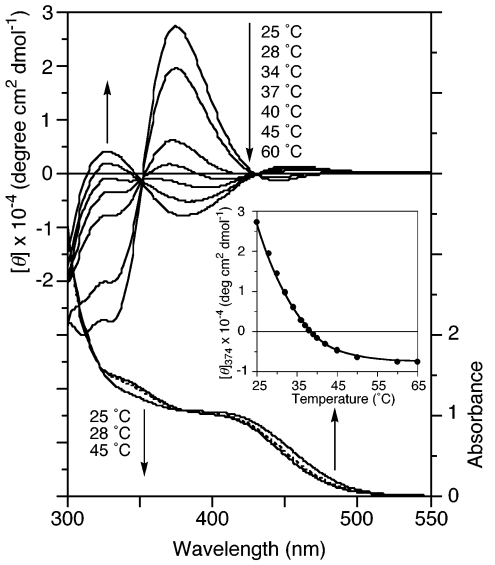

Figure 4. CD and absorption spectral changes of poly(*R*)-**1** (run 1 in Table 1) (1 mg/mL) in DMF with temperature. Inset: plots of the molar ellipticity at 374 nm ($[\theta]_{374}$) for poly-(*R*)-**1** vs temperature.

Besides solvents, poly-**1**'s were found to respond to temperature and exhibited a similar temperature-driven helix inversion in DMF. Figure 4 shows the changes in the CD and absorption spectra of poly(*R*)-**1** in DMF with temperature as an example. The CD pattern dramatically changed at high temperatures, and the sign inverted through a transition temperature ($[\theta]$ of the Cotton effects ≈ 0 at around $T_m = 37$ °C) with clear isosbestic points (($[\theta]$ of the Cotton effects ≈ 0 at 352 and 430 nm) to give an almost mirror image at 60 °C. The right- and left-handed helices of poly(*R*)-**1** are not exactly enantiomers, but diastereomers due to the presence of chiral naphthylethylcarbamoyl residues of poly(*R*)-**1**, and therefore, their CD spectra differ from one another.[19] These ICD changes were accompanied by a slight red shift in the absorption spectra with isosbestic points at 323 and 381 nm. These CD and absorption spectral changes are reversible and independent of the poly(*R*)-**1** concentration (0.025−1.0 mg/mL) and time, indicating that the formation of aggregates depending on the temperature could be excluded. Poly(*S*)-**1** also showed the same CD changes with temperature. These results suggest that the poly-**1**'s undergo a thermodriven helix−helix transition.

Controlling or switching the helix-sense of macromolecules using chiral stimuli is quite interesting but still a very difficult task.[8,9] We found that the poly(*R*)-**1** and poly(*S*)-**1** also underwent the helix−helix transition in DMF in the presence of a chiral amine, (*R*)-(+)- and (*S*)-(−)-1-(1-naphthyl)ethylamine ((*R*)- and (*S*)-**2**). Figure 5 shows the CD spectra of poly(*R*)-**1** in the presence of (*R*)- and (*S*)-**2** in DMF. The ICD changed with an increase in the concentration of (*R*)-**2**; the CD intensity at 374 nm decreased, and the sign inverted to give an almost mirror image at [**2**]/[poly(*R*)-**1**] = 400 (see Figure 5B). These changes in the ICDs were accompanied by only minor changes in the UV−vis absorption spectra; a peak around 400 nm in the UV−vis spectrum of poly-(*R*)-**1** slightly shifted to a longer wavelength by ca. 5 nm in the presence of 500-fold **2**. The ICD of poly(*R*)-**1** also changed in the presence of excess (*S*)-**2**, but the changes with (*R*)-**2** are remarkable. Thus, **2** can be used to regulate the helicity of poly(*R*)-**1**. Similar CD changes

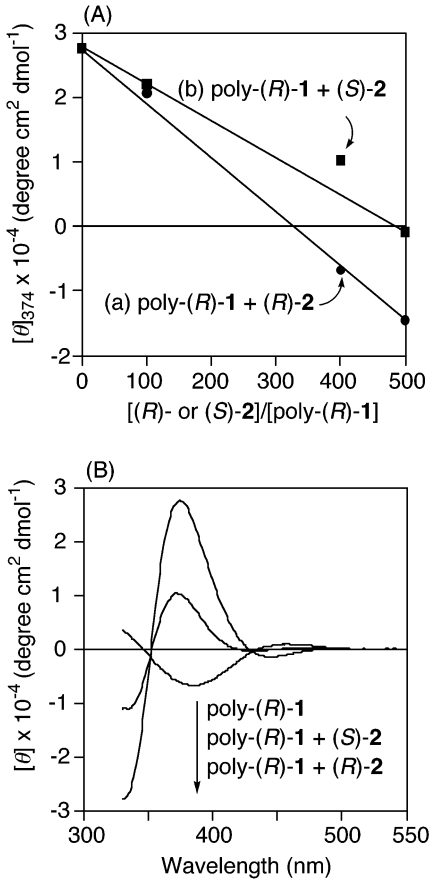

Figure 5. Plots of CD intensity at 374 nm for poly(*R*)-**1** (run 1 in Table 1) (1 mg/mL) vs the concentration of (*R*)-**2** (a) and (*S*)-**2** (b) (A) in DMF at ambient temperature (ca. 25−26 °C). The CD spectra of poly(*R*)-**1** at [**2**]/[poly(*R*)-**1**] = 0 and 400 are also shown in (B).

were also observed for poly(*S*)-**1** in the presence of the same chiral amines ($[\theta]_{2nd} \times 10^{-4}$ (deg cm^2 dmol^{-1}) of poly(*S*)-**1** with (*R*)-**2** and (*S*)-**2** ([**2**]/[poly(*S*)-**1**] = 400) = −1.06 and +0.82, respectively) (see also Supporting Information).

For the poly(phenylacetylene) with a chiral norephedrine group, the binding with a small amount of (*R*)-mandelic acid induced a dramatic change in the ICD of the polymer in solution due to the helix−helix transition through a rather strong acid−base interaction.[8] On the other hand, the main interaction of poly-**1**'s with **2** may be hydrogen bonding, and such interaction is not strong enough so that excess (*R*)-**2** or (*S*)-**2** should be necessary for the helix inversion of the polymers. The helical structures of the poly-**1**'s are sensitive to temperature as well as to the chirality of the chiral amines as mentioned above. We then measured the changes in the CD spectra of the poly(*R*)-**1**−**2** complexes ([**2**]/[poly(*R*)-**1**] = 400, see Figure 5) in DMF at various temperatures (Figure 6). As expected, the poly(*R*)-**1**−(*S*)-**2** complex showed completely reversible inversion of the Cotton effect sign at high temperature and exhibited a similar CD as the poly(*R*)-**1**−(*R*)-**2** complex.[20] At lower temperatures, however, both complexes showed the same Cotton effect signs. The helix-senses of the complexes are determined in a delicate fashion that is balanced by temperature, additives, and solvents.

We conclude that optically active poly(phenylacetylenes), poly(*R*)-**1** and poly(*S*)-**1**, exhibit a unique helix−helix transition by response to achiral and chiral

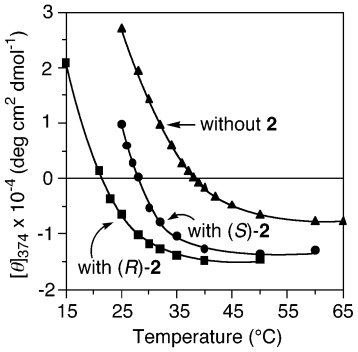

Figure 6. Plots of the molar ellipticity at 374 nm ($[\theta]_{374}$) for poly(*R*)-**1** (run 1 in Table 1) (1 mg/mL) vs temperature in the absence and presence of **2** in DMF. [**2**]/[poly(*R*)-**1**] = 400.

stimuli. We expect that related optically active poly(phenylacetylenes) bearing other chiral substituents would also respond, for example, to chiral amines or sugars, showing a characteristic helix−helix transition depending on the chirality of the molecules.

Acknowledgment. We thank Professor K. Kobayashi (Nagoya University) for permission to use the DLS apparatus. We also acknowledge T. Asari (Nagoya University) for his experimental assistance. This work was partially supported by Grant-in-Aid for Scientific Research from Japan Society for the Promotion of Science and the Ministry of Education, Culture, Sports, Science, and Technology, Japan.

Supporting Information Available: Experimental procedures for AFM and DLS measurements, AFM images of poly(*R*)-**1**, plots of the CD intensity of poly(*R*)-**1** vs temperature in the absence and presence of (*R*)-**2**, (*S*)-**2**, (*RS*)-**2**, and benzylamine in DMF, and CD spectral data of poly(*R*)-**1** and poly(*S*)-**1** in the presence of (*R*)- and (*S*)-**2** in DMF. This material is available free of charge via the Internet at http://pubs.acs.org.

References and Notes

(1) For reviews of helical polymers and oligomers (foldamers), see: (a) Okamoto, Y.; Nakano, T. *Chem. Rev.* **1994**, *94*, 349−372. (b) Green, M. M.; Peterson, N. C.; Sato, T.; Teramoto, A.; Cook, R.; Lifson, S. *Science* **1995**, *268*, 1860−1866. (c) Gellman, S. H. *Acc. Chem. Res.* **1998**, *31*, 173−180. (d) Green, M. M.; Park, J.-W.; Sato, T.; Teramoto, A.; Lifson, S.; Selinger, R. L. B.; Selinger, J. V. *Angew. Chem., Int. Ed.* **1999**, *38*, 3138−3154. (e) Srinivasarao, M. *Curr. Opin. Colloid Interface Sci.* **1999**, *4*, 370−376. (f) Fujiki, M. *Macromol. Rapid Commun.* **2001**, *22*, 539−563. (g) Hill, D. J.; Mio, M. J.; Prince, R. B.; Hughes, T. S.; Moore, J. S. *Chem. Rev.* **2001**, *101*, 3893−4011. (h) Okamoto, Y.; Nakano, T. *Chem. Rev.* **2001**, *101*, 4013−4038. (i) Conrnelissen, J. J. L. M.; Rowan, A. E.; Nolte, R. J. M.; Sommerdijk, N. A. J. M. *Chem. Rev.* **2001**, *101*, 4039−4070. (j) Brunsveld, L.; Folmer, B. J. B.; Meijer, E. W.; Sijbesma, R. P. *Chem. Rev.* **2001**, *101*, 4071−4097.

(2) (a) Yashima, E.; Matsushima, T.; Okamoto, Y. *J. Am. Chem. Soc.* **1995**, *117*, 11596−11597. (b) Yashima, E.; Nimura, T.; Matsushima, T.; Okamoto, Y. *J. Am. Chem. Soc.* **1996**, *118*, 9800−9801. (c) Yashima, E.; Maeda, Y.; Okamoto, Y. *Chem. Lett.* **1996**, 955−956. (d) Yashima, E.; Matsushima, T.; Okamoto, Y. *J. Am. Chem. Soc.* **1997**, *119*, 6345−6359. (e) Yashima, E.; Maeda, Y.; Matsushima, T.; Okamoto, Y. *Chirality* **1997**, *9*, 593−600. (f) Yashima, E.; Goto, H.; Okamoto, Y. *Polym. J.* **1998**, *30*, 69−71. (g) Saito, M. A.; Maeda, K.; Onouchi, H.; Yashima, E. *Macromolecules* **2000**, *33*, 4316−4318. (h) Maeda, K.; Goto, H.; Yashima, E. *Macromolecules* **2001**, *34*, 1160−1164. (i) Kawamura, H.; Maeda, K.; Okamoto, Y.; Yashima, E. *Chem. Lett.* **2001**, 58−59. (j) Onouchi, H.; Maeda, K.; Yashima, E. *J. Am. Chem. Soc.* **2001**, *123*, 7441−7442.

(3) Yashima, E.; Maeda, K.; Okamoto, Y. *Nature (London)* **1999**, *399*, 449−451.

(4) For helix−helix transition of biopolymers: (a) Schulz, G. E.; Schirmer, R. H. *Principles of Protein Structure;* Springer-Verlag: New York, 1979; Chapter 5. (b) Saenger, W. *Principles of Nucleic Acid Structure;* Springer-Verlag: New York, 1984; Chapter 12. (c) Kurtz, J.; Berger, A.; Katchalski, E. *Nature (London)* **1956**, *178*, 1066−1067. (d) Blout, E. R.; Carver, J. P.; Gross, J. *J. Am. Chem. Soc.* **1963**, *85*, 644−646. (e) Bradbury, E. M.; Carpenter, B. G.; Goldman, H. *Biopolymers* **1968**, *6*, 837−850. (f) Overberger, C. G.; David, K.-H. *Macromolecules* **1972**, *5*, 373−377. (g) Pohl, F. M.; Jovin, T. M. *J. Mol. Biol.* **1972**, *67*, 375−396. (h) Matsumoto, M.; Watanabe, H.; Yoshioka, K. *Biopolymers* **1973**, *12*, 1729−1739. (i) Ebert, C.; Ebert, G. *Colloid Polym. Sci.* **1977**, *255*, 1041−1053. (j) Toriumi, H.; Saso, N.; Yasumoto, Y.; Sasaki, S.; Uematsu, I. *Polym. J.* **1979**, *11*, 977−981. (k) Ueno, A.; Takahashi, K.; Anzai, J.; Osa, T. *J. Am. Chem. Soc.* **1981**, *103*, 6410−6415. (l) Ciardelli, F.; Pieroni, O.; Fissi, A.; Carlini, C.; Altomare, A. *Br. Polym. J.* **1989**, *21*, 97−106. (m) Watanabe, J.; Okamoto, S.; Abe, A. *Liq. Cryst.* **1993**, *15*, 259−263. (n) Watanabe, J.; Okamoto, S.; Satoh, K.; Sakajiri, K.; Furuya, H. *Macromolecules* **1996**, *29*, 7084−7088. (o) Mahadevan, S.; Palaniandavar, M. *Chem. Commun.* **1996**, 2547−2548. (p) Boiadjiev, S. E.; Lightner, D. A. *J. Am. Chem. Soc.* **2000**, *122*, 378−383.

(5) For helix−helix transition of synthetic polymers by solvents: (a) Okamoto, Y.; Nakano, T.; Ono, E.; Hatada, K. *Chem. Lett.* **1991**, 525−528. (b) Cheuk, K. K. L.; Salhi, F.; Lam, J. W. Y.; Tang, B. Z. *Polym. Prepr.* **2000**, *41* (2), 1567−1568.

(6) For helix−helix transition of synthetic polymers by temperatures: (a) Maeda, K.; Okamoto, Y. *Macromolecules* **1998**, *31*, 5164−5166. (b) Maeda, K.; Okamoto, Y. *Macromolecules* **1999**, *32*, 974−980. (c) Hino, K.; Maeda, K.; Okamoto, Y. *J. Phys. Org. Chem.* **2000**, *13*, 361−367. (d) Cheon, K. S.; Selinger, J. V.; Green, M. M. *Angew. Chem., Int. Ed.* **2000**, *39*, 1482−1485. (e) Fujiki, M. *J. Am. Chem. Soc.* **2000**, *122*, 3336−3343. (f) Koe J. R.; Fujiki, M.; Motonaga, M.; Nakashima, H. *Chem. Commun.* **2000**, 389−390. (g) Fujiki, M.; Koe J. R.; Motonaga, M.; Nakashima, H.; Terao, K.; Teramoto, A. *J. Am. Chem. Soc.* **2001**, *123*, 6253−6261. (h) Nakako, H.; Nomura, R.; Masuda, T. *Macromolecules* **2001**, *34*, 1496−1502.

(7) For helix−helix transition of synthetic polymers by light, see ref 4l and (a) Maxein, G.; Zentel, R. *Macromolecules* **1995**, *28*, 8438−8440. (b) Mayer, S.; Maxein, G.; Zentel, R. *Macromolecules* **1998**, *31*, 8522−8525.

(8) Yashima, E.; Maeda, Y.; Okamoto, Y. *J. Am. Chem. Soc.* **1998**, *120*, 8895−8896.

(9) Yashima, E.; Maeda, K.; Sato, O. *J. Am. Chem. Soc.* **2001**, *123*, 8159−8160.

(10) (a) Furlani, A.; Napoletano, C.; Russo, M.; Camus, A.; Marsich, N. *J. Polym. Sci., Polym. Chem. Ed.* **1989**, *27*, 75−86. (b) Tabata, M.; Yang, W.; Yokota, K. *Polym. J.* **1990**, *12*, 1105−1107.

(11) (a) Simionescu, C.; Dumitrescu, S.; Percec, V. *J. Polym. Sci., Polym. Symp.* **1978**, *64*, 209−227. (b) Furlani, A.; Napoletano, C.; V. Russo, M. V.; Feast, W. J. *Polym. Bull. (Berlin)* **1986**, *16*, 311−317. (c) Kishimoto, Y.; Eckerle, P.; Miyatake, T.; Kainosho, M.; Ono, A.; Ikariya, T.; Noyori, R. *J. Am. Chem. Soc.* **1999**, *94*, 8897−8909.

(12) (a) Shirakawa, H.; Ito, T.; Ikeda, S. *Polym. J.* **1973**, *4*, 469−462. (b) Harada, I.; Tasumi, M.; Shirakawa, H.; Ikeda, S. *Chem. Lett.* **1978**, 1411−1414. (c) Tabata, M.; Tanaka, Y.; Sadahiro, Y.; Sone, T.; Yokota, K.; Miura, I. *Macromolecules* **1997**, *30*, 5200−5204.

(13) (a) Yashima, E.; Huang, S.; Okamoto, Y. *J. Chem. Soc., Chem. Commun.* **1994**, 1811−1812. (b) Yashima, E.; Huang, S.; Matsushima, T.; Okamoto, Y. *Macromolecules* **1995**, *28*, 4184−4193. (c) Yashima, E.; Matsushima, T.; Nimura, T.; Okamoto, Y. *Korean Polym. J.* **1996**, *4*, 139−146. (d) Yashima, E. *Anal. Sci.* **2002**, *18*, 3−6.

(14) (a) Bouman, M. M.; Havinga, E. E.; Janssen, R. A. J.; Meijer, E. W. *Mol. Cryst. Liq. Cryst.* **1994**, *256*, 439−448. (b) Pu, L. *Acta Polym.* **1997**, *48*, 116−141. (c) Yashima, E.; Goto, H.; Okamoto, Y. *Macromolecules* **1999**, *32*, 7942−7945. (d) Zhang, Z.-B.; Fujiki, M.; Motonaga, M.; Nakashima, H.; Torimitsu, K.; Tang, H.-Z. *Macromolecules* **2002**, *35*, 941−944. (e) Goto,

H.; Yashima, E. *J. Am. Chem. Soc.* **2002**, *124*, 7943−7949. (f) Goto, H.; Okamoto, Y.; Yashima, E. *Chem. Eur. J.* **2002**, *8*, 4027−4036.
(15) Guenet, J.-M.; Jeon, H. S.; Khatri, C.; Jha, S. K.; Balsara, N. P.; Green, M. M.; Brulet, A.; Thiery, A. *Macromolecules* **1997**, *30*, 4590−4596.
(16) (a) Yamamoto, T.; Komarudin, D.; Arai, M.; Lee, B.-L.; Suganuma, H.; Asakawa, N.; Inoue, Y.; Kubota, K.; Sasaki, S.; Fukuda, T.; Matsuda, H. *J. Am. Chem. Soc.* **1998**, *120*, 2047−2058. (b) Goto, H.; Okamoto, Y.; Yashima, E. *Macromolecules* **2002**, *35*, 4590−4601.
(17) We also measured DLS of poly-(*S*)-**1** (run 4 in Table 1) in DMF and DMF−pyridine (1/9, v/v). The estimated hydrodynamic radius (R_h) value of the polymer in DMF−pyridine (1/9) (28 nm) was almost the same as that measured in DMF (33 nm). These DLS results also support this conclusion (see Supporting Information).
(18) Sakurai, S.; Kuroyanagi, K.; Yashima, E., unpublished results. Also see: Ishikawa, M.; Maeda, K.; Yashima, E. *J. Am. Chem. Soc.* **2002**, *124*, 7448−7458.
(19) In this case, loss of helicity or incomplete inversion of the helix sense should be taken into consideration for the observed weak Cotton effects at high temperatures compared with those at low temperatures.
(20) In this case, chiral solvation effect should be also taken into consideration for the observed CD changes, since poly-(*R*)-**1** showed inversion of the Cotton effect sign at high temperature even in the presence of racemic **2** ((*RS*)-**2**) and achiral benzylamine (see Supporting Information). However, the difference in the ICD changes of poly-(*R*)-**1** with (*R*)- and (*S*)-**2** at different temperature indicates that chirality of **2** contributes to the inversion to some extent.

MA025726P